J Appl Physiol 96: 1600–1605, 2004.
First published January 5, 2004; 10.1152/japplphysiol.00595.2003.

Rheology of airway smooth muscle cells is associated with cytoskeletal contractile stress

Dimitrije Stamenović,[1] Béla Suki,[1] Ben Fabry,[2] Ning Wang,[2] and Jeffrey J. Fredberg[2]
(With the Technical Assistance of Julie E. Buy[1])
[1]*Department of Biomedical Engineering, Boston University, and* [2]*Physiology Program, Harvard School of Public Health, Boston, Massachussetts 02115*

Submitted 10 June 2003; accepted in final form 31 December 2003

Stamenović, Dimitrije, Béla Suki, Ben Fabry, Ning Wang, and Jeffrey J. Fredberg. Rheology of airway smooth muscle cells is associated with cytoskeletal contractile stress. *J Appl Physiol* 96: 1600–1605, 2004. First published January 5, 2004; 10.1152/japplphysiol.00595.2003.—Recently reported data from mechanical measurements of cultured airway smooth muscle cells show that stiffness of the cytoskeletal matrix is determined by the extent of static contractile stress borne by the cytoskeleton (Wang N, Tolić-Nørrelykke IM, Chen J, Mijailovich SM, Butler JP, Fredberg JJ, and Stamenović D. *Am J Physiol Cell Physiol* 282, C606–C616, 2002). On the other hand, rheological measurements on these cells show that cytoskeletal stiffness changes with frequency of imposed mechanical loading according to a power law (Fabry B, Maksym GN, Butler JP, Glogauer M, Navajas DF, and Fredberg JJ. *Phys Rev Lett* 87: 148102, 2001). In this study, we examine the possibility that these two empirical observations might be interrelated. We combine previously reported data for contractile stress of human airway smooth muscle cells with new data describing rheological properties of these cells and derive quantitative, mathematically tractable, and experimentally verifiable empirical relationships between contractile stress and indexes of cell rheology. These findings reveal an intriguing role of the contractile stress: although it maintains structural stability of the cell under applied mechanical loads, it may also regulate rheological properties of the cytoskeleton, which are essential for other cell functions.

contractility; power law; stiffness; cytometry; mechanics

WE ATTEMPT HERE to bring together two empirical observations concerning the deformability of the cytoskeleton (CSK) of adherent cells. On the one hand, Wang et al. (25) have shown that the stiffness of the CSK matrix of cultured human airway smooth muscle (HASM) cells depends mainly on the static contractile stress that is borne by the CSK microfilaments and varies with that contractile stress in a linear fashion. The greater the contractile stress, the stiffer the cell is. Although other interpretations are possible, such a finding is consistent with the idea that the CSK behaves mechanically mainly as a tensed cable network (25). In that case, elastic restoring forces arise mainly from changes in the orientation and spacing of tensed filaments as the network is deformed (cf. Refs. 19, 21). The contribution of this mechanism to the matrix stiffness is a consequence of the internal balance of forces. This simple mechanism is not mutually exclusive with other factors that might add to CSK stiffness, but it sets a firm lower bound on that stiffness. Interestingly, in HASM cells, this lower bound seems to account for most of the observed stiffness (25).

On the other hand, Fabry et al. (6, 7) have established that the stiffness (as well as other rheological properties) of the CSK matrix of cultured HASM cells increases with frequency of the imposed deformation as a weak power law, ω^{α}, where ω is loading frequency and α is the power-law exponent ($0 \leq \alpha \leq 1$). This power-law behavior extends over five decades of frequency (10^{-2}–10^{3} Hz) and persists over a wide range of experimental conditions. As explained below, α is an index of transition between solid-like ($\alpha = 0$) and Newtonian fluid-like ($\alpha = 1$) behaviors. Fabry et al. (6) recognized that this power-law behavior conforms to what is known in the engineering literature as structural (hysteretic) damping, an empirical law suggesting that the phase lag between the frictional and elastic stresses that develop within a material body is independent of the frequency of the loading (cf. Refs. 8, 13). Although the mechanistic basis of this behavior remains unclear, these data rule out viscoelastic models with one or even several time constants, as well as the structural assumptions and dynamics on which such models rest. For example, data of Fabry et al. (6, 7) rule out the Voigt model, the Maxwell model, and the standard linear solid model. In addition, the studies by Fabry et al. (6, 7) showed a substantial range of linear responses and no yield stress in various types of adherent cells, thereby ruling out, as well, Bingham-type plastic behavior (1) as well as so-called power-law fluids (12). On the other hand, observations of Fabry et al. (6, 7) are consistent with the hypothesis that the ability of the CSK to deform, to flow, and to remodel corresponds to the behavior of soft glassy materials existing close to a glass transition (18).

In this study, we examine the possibility that these two empirical observations (linear dependence of the stiffness on the static contractile stress and power-law dependence of the stiffness on the frequency of the imposed loading) might be interrelated. We address the extent to which these observations are compatible and complementary or contradictory. We combine previously reported data for contractile stress of HASM cells (25) with new data describing rheological properties of HASM cells and derive quantitative, mathematically tractable, and experimentally verifiable empirical relationships between contractile stress and indexes of cell rheology. Tentative mechanistic interpretations of these findings are discussed.

METHODS

We used our previously reported data for contractile stress measured in cultured HASM cells in response to graded doses of hista-

Address for reprint requests and other correspondence: D. Stamenović, Dept. of Biomedical Engineering, Boston Univ., 44 Cummington St., Boston, MA 02215 (E-mail: dimitrij@engc.bu.edu).

The costs of publication of this article were defrayed in part by the payment of page charges. The article must therefore be hereby marked "*advertisement*" in accordance with 18 U.S.C. Section 1734 solely to indicate this fact.

mine and isoproterenol (25). We measured rheological properties of cultured HASM cells in which contractility was modulated by agonists and doses that matched those that were used in the previous measurements of contractile stress. We then combined those two sets of data and derived empirical relationships between the contractile stress and indexes of cell rheology. A brief description of cell culture and rheological measurements are given below.

Cell culture. Cells were isolated from tracheal muscle of human lung transplant donors (approved by the University of Pennsylvania Committee on Studies Involving Human Subjects) as described previously (15). Cells at *passages 3–6* were used in all experiments. These cells maintain smooth muscle morphology and physiological responsiveness to agonists until at least *passage 8*. After cells reached confluence in plastic dishes, they were serum deprived for 48 h before being trypsinized. The cells were then plated in a serum-free medium on collagen I-coated (0.2 mg/ml) wells (96-well plate, Immunon II, Dynetec) at a density of 20,000 cells/well.

Magnetic oscillatory cytometry. Detailed description and validation of this technique is given elsewhere (6, 7). Briefly, small (4.5-μm diameter) ferrimagnetic beads were coated with RGD (Arg-Gly-Asp) peptide, which binds specifically to integrin receptors on the cell apical surface. Beads were added for 20 min to cells plated for 4–6 h on the collagen I-coated wells. Unbound beads were removed by washing with a serum-free medium, and then oscillatory measurements were performed as follows. The beads (1 bead/cell on average) were first magnetized by horizontal magnetic field and then twisted by a sinusoidally varying ($\sim 10^{-1}$–10^3 Hz) vertical magnetic field. The horizontal displacements of each bead were traced by a charge-coupled device camera (JAI CV-M10) mounted on an inverted microscope.

Protocol. We started by measuring the frequency response of HASM cells between $\sim 10^{-1}$ and $\sim 10^3$ Hz twice, first in an ascending order and then in a descending order. We then recorded the cell response continuously at 0.75 Hz while adding an agonist to the well (0.1 and 10 μM isoproterenol, and 10 μM histamine or sham). This was done to ensure that the cells responded to the agonists. Our laboratory showed previously (25) that 10 μM is a saturating dose for both agonists, and thus they achieve a wide range of contractility in HASM cells. Fifteen minutes after adding the agonists, we again measured the cell frequency response between $\sim 10^{-1}$ and $\sim 10^3$ Hz twice. All measurements were repeated in five cell wells. We analyzed the displacements of ~120–150 beads from each well. Beads that displaced by >500 nm or moved at an angle of >45° relative to the magnetization direction were discarded. For each bead, we computed an apparent complex modulus as the ratio between specific torque (amplitude order of 10^1 Pa) and bead displacement (order of 10^2 nm). This value had dimensions of (force/area)/length and was then transformed into a traditional dynamic (complex) modulus G^* (dimensions force/area) by multiplication with a geometric factor that depends on the shape and thickness of the cell and on the degree of bead internalization in the cell (14). The real part of G^* is the elastic (storage) modulus (G'), and the imaginary part is the frictional (loss) modulus (G''). For each tested frequency, median values of G' and G'' were found and averaged over four (2 ascending and 2 descending) runs. This procedure was repeated for each of the five wells, and the mean values of G' and G'' were obtained for each frequency and each cell treatment.

The structural damping equation (*Eq. 1*) was fit to these data

$$G^* = G_0\left(\frac{\omega}{\Phi_0}\right)^{\alpha}(1 + i\eta)\cos\frac{\alpha\pi}{2} + i\mu\omega \qquad (1)$$

where G_0 and Φ_0 are scale factors for stiffness and frequency, respectively, $\eta = \tan(\alpha\pi/2)$ has been called the structural damping coefficient (cf. 13), μ is the viscous damping coefficient, and $i = \sqrt{-1}$ indicates the out-of-phase behavior. G', which corresponds to the real part of *Eq. 1*, increases for all frequencies ω according to a power law with exponent α. G'', which corresponds to the imaginary part of *Eq. 1*, includes a component that also increases as a power law with the same exponent. Therefore, this component is a frequency-independent fraction (η) of G'; such a direct coupling of G' and G'' is the characteristic feature of structural damping behavior (8). G'' also includes a Newtonian viscous term, $\mu\omega$, which turns out to be small except at very high frequencies. In the limit of $\alpha \to 0$, $G' \to G_0$ and $\eta \to 0$; i.e., elastic solid behavior. In the limit of $\alpha \to 1$, G'' becomes proportional to ω and $\eta \to \infty$, i.e., Newtonian fluid behavior. Thus *Eq. 1* describes a relationship between changes of the exponent of the power law and the transition from solid-like ($\alpha = 0$, $\eta = 0$) to Newtonian fluid-like ($\alpha = 1$, $\eta = \infty$) behavior. The Newtonian viscous term $\mu\omega$ in *Eq. 1* should not be confused with the Newtonian fluid behavior in the limit when $\alpha = 1$. This term indicates the prevailing behavior of G'' at very high frequencies regardless of what value α has.

Data analysis. The fitting of *Eq. 1* to the oscillatory data was done by a least-squares method by minimizing the squared differences between $\log G^*$ of the data and of the model summed over all frequencies and all drug treatment conditions, with the constraint that G_0 and Φ_0 remain constant for all cell treatments (5). The values of α and μ were free to vary with cell treatment. The reason for keeping G_0 and Φ_0 fixed was that they represent coordinates of the approximate point of intersection of the G' vs. ω curves (see RESULTS). The minimization was performed using Microsoft Excel solver. We analyzed the sensitivity of the fit of *Eq. 1* to variability (noise) in the data by determining the 95% confidence interval of the parameter estimates using a previously described method (5).

RESULTS

The elastic modulus G' increased with increasing frequency ω according to a weak power law over the observed frequency range (10^{-1}–10^3 Hz) (Fig. 1*A*). On a log-log scale, the power-law dependence has a linear appearance with the slope being equivalent to the power-law exponent α. The frictional modulus G'' also followed the weak power law initially (10^{-1}–10 Hz), but above 10 Hz the frequency dependence became progressively stronger (Fig. 1*B*). The power-law behavior persisted after agonist treatment, although the exponent α changed. In histamine-treated cells, both G' and G'' increased while their dependences on ω decreased relative to the control conditions. In isoproterenol-treated cells, both G' and G'' decreased while their dependences on ω increased relative to the control conditions in a dose-dependent fashion (Fig. 1). When extrapolated to high frequencies, the G' vs. ω relationships intersected at an approximately common fixed point (Fig. 1*A*, *inset*). All these observations are consistent with the previously reported data for HASM cells (6).

The structural damping equation (*Eq. 1*) provided an excellent fit to the oscillatory data (Fig. 1). We obtained a unique set of values for G_0 and Φ_0, whereas the values for α and μ depended on cell treatment (Table 1). The exponent α exhibited a systematic dependence on the cell treatment. In stimulated cells, α decreased, whereas in relaxed cells α gradually increased relative to the controls with increasing doses of isoproterenol. This, in turn, suggests that rheological behavior of stimulated cells is closer to the behavior of an elastic solid than that of relaxed cells. The μ changed with cell treatment, but these changes were not systematic and were considerably smaller than those of G' or G'' measured at low frequencies, suggesting that the state of cell contractility has little effect on μ.

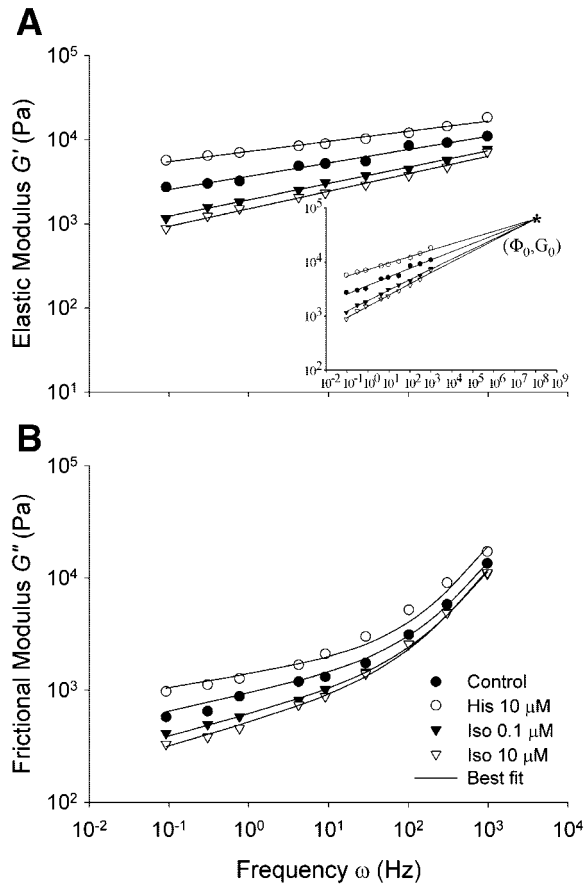

Fig. 1. *A*: elastic modulus (G') in human airway smooth muscle (HASM) cells increased with increasing frequency (ω) according to a weak power law for different agonist cell treatments. *Inset*: when extrapolated to high frequencies, G' vs. ω curves converged at an approximate common point of intersection with coordinates (Φ_0, G_0). *B*: frictional modulus (G'') also increased according to the weak power law up to 10 Hz, but above 10 Hz the power-law dependence increased. Measurements were done using the magnetic oscillatory technique under control conditions after treatment with histamine (His; 10 μM) and isoproterenol (Iso; 0.1 and 10 μM). Data points are means; SE does not exceed 5% of the means (not shown). Solid lines are fit of *Eq. 1* to the data.

To establish whether there exists a fixed empirical relationship between G' and G'' on the one hand and the active stress (P) on the other, we combined the oscillatory data with previously published data for P as a function of doses of histamine and isoproterenol (25). P was obtained from the Fourier transform traction microscopy technique (3, 25). This technique measures traction that arises at the interface of a cell and a flexible substrate in response to cell contraction (Fig. 2*A*). Because traction balances contractile stress (20, 25), the latter can be computed from traction measurements (Fig. 2*B*). It was found that P increases or decreases in a dose-dependent fashion relative to the control conditions after histamine or isoproterenol were added (Fig. 2*C*). By cross-plotting these data and the oscillatory data (Fig. 1), we obtained that at each frequency both G' and G'' increased with increasing P (Fig. 3). We chose to examine the behavior at low frequencies ($\sim$0.1 Hz). The reason for selecting the lowest frequency from the measured range of frequencies is the mathematical simplicity of the G' vs. P relationship at low frequencies. For reasons explained in DISCUSSION, this selection had no effect on the results we obtained. We found that, at 0.1 Hz, G' conforms to a simple, proportional dependence on P (Fig. 3*A*, *inset*), which was consistent with our previous result in HASM cells (25)

$$G' = cP \tag{2}$$

where $c = 2.96$ is a factor of proportionality whose value was determined from the slope of the linear regression line (Fig. 3*A*, *inset*).

Compatibility between frequency- and stress-dependent behavior. For *Eqs. 1* and *2* to be mathematically consistent at 0.1 Hz′ the real part of *Eq. 1* has to be equal to the right-hand side of *Eq. 2*, i.e.,

$$cP = G_0\left(\frac{0.1}{\Phi_0}\right)^{\alpha}\cos\frac{\alpha\pi}{2} \tag{3}$$

Since $\Phi_0 = 4.07 \times 10^7$ Hz (Table 1), it follows from *Eq. 3* that P decreases as α increases from 0 to 1. The α vs. P relationship was calculated from *Eq. 3* by taking values of $G_0 = 6.09 \times 10^4$ Pa, $\Phi_0 = 4.07 \times 10^7$ Hz, and $c = 2.96$. The relationship of α vs. P obtained in this way was consistent with experimental data (Fig. 4), where P was obtained from the traction measurements (Fig. 2*C*) and the corresponding values for α from the log-log slope of the G' vs. ω relationships (Fig. 1*A* and Table 1). It is important to note that, although the α vs. P relationship (*Eq. 3*) was derived at 0.1 Hz, it is not limited to this particular frequency because neither α nor P are frequency-dependent variables. Thus α depends only on P and nothing else. The contractile stress alone determined cell transition between solid-like ($\alpha = 0$) and fluid-like ($\alpha = 1$) behavior.

To test the consistency of this α vs. P relationship with other experimental data, we derived from *Eqs. 1* and *3* G' vs. P and G'' vs. P relationships for different frequencies (Fig. 5) and compared them with the corresponding experimental data (Fig. 3). Because μ varied little with the cell treatments (Table 1), we took the average $\mu = 1.83$ Pa·s of the values from Table 1 when calculating the G'' vs. P relationships. Relationships of G' vs. P and G'' vs. P computed in this way were consistent with experimental data (Fig. 5).

DISCUSSION

Cellular functions demand a trade-off between deformability on the one hand and mechanical robustness on the other (4). Under certain conditions (e.g., crawling, spreading, division, invasion), cells need to be highly deformable, almost fluid like, whereas to maintain their structural integrity cells have to behave as an elastic solid. Our results establish a novel empirical relationship between an index of transition from solid-like to fluid-like cell behavior on the one hand and the contractile

Table 1. *Estimated parameter values*

Treatment	G_0, kPa	Φ_0, Hz	α	μ, Pa·s
Control	60.9±38.4	4.07±7.07 × 10^7	0.158±0.008	1.76±0.27
10 μM His			0.121±0.012	2.55±0.38
0.1 μM Iso			0.194±0.009	1.46±0.21
10 μM Iso			0.208±0.011	1.55±0.21

Parameter values G_0, Φ_0, α, and μ (means ± 3 SE) were obtained by fitting *Eq. 1* to the oscillatory data in Fig. 1, *A* and *B*. Values of G_0 and Φ_0 are the same for all cell treatments. His, histamine treatment; Iso, isoproterenol treatment.

mechanical stress borne by the CSK on the other (*Eq. 3*; Fig. 4). This relationship has not been tied to any theoretical model of cell rheological behavior, nor does it assume any particular biophysical or biochemical mechanism; it represents pure empiricisms, the physical basis of which remains to be explained. Before discussing potential mechanisms, we critically evaluate our findings.

According to *Eq. 1*, the complex modulus G^* tends toward zero as the frequency ω tends toward zero, which is a characteristic of fluids. That is, at long time scales, there is no "spring constant"; all elastic behavior is lost, and force is dissipated by flow. However, this is true only when α is greater than zero. When $\alpha = 0$, by contrast, $G^* = G' = G_0 =$ constant for all ω, which, in turn, is indicative of solid-like behavior and corresponds to a static elastic limit. Moreover, according to *Eq. 3*, for $\alpha = 0$, $G_0 = cP$, i.e., the elastic modulus is determined by the level of the CSK contractile stress. This feature is consistent with the behavior of tensed cable networks, including tensegrity, which we used in our previous studies as a model of CSK elasticity (cf. Refs. 19, 21). However, taking into account that $G_0 \approx 61$ kPa (Table 1) and $c \approx 3$, it follows that P, corresponding to the elastic limit of $\alpha = 0$, would be an order of magnitude greater than the highest value of P measured in HASM cells treated with the saturating dose of histamine (Fig. 2*C*). Thus, in the physiological range of P, the HASM cell most likely does not attain the elastic limit. At the same time, it comes close to that limit in the sense that the observed range of α is 0.1–0.2. Therefore, in the spectrum of possible behaviors, with 0 corresponding to the limit of a Hookean elastic solid and 1 corresponding to the limit of a Newtonian fluid, these cells are closer to the former than the latter.

A concern could be raised that the direct proportionality between G' and P at 0.1 Hz (*Eq. 2*) was established on the basis of only four data points (Fig. 3*A*, *inset*). However, in a previous study (25), our laboratory obtained a very similar relationship with twice as many data points. Thus, at low frequencies, the proportionality between G' and P seems to be realistic. At higher frequencies, however, this proportionality ceases and the G' vs. P relationship becomes nonlinear (Fig. 5*A*). Nevertheless, G' collapses to zero when $P = 0$ at all frequencies (Fig. 5*A*). This, in turn, suggests that the contractile stress is a key determinant of the CSK shape stability not only under quasi-static conditions but under dynamic conditions as well.

Another concern is that the oscillatory data (Fig. 1) may not be a reflection of mechanics of the CSK but instead are attributable to the probe we used, receptor kinetics, or membrane mechanics. These issues are critically evaluated in the recent publication of Fabry et al. (7). The evidence they provided argues against those possibilities.

Mechanistic interpretation. It is often assumed that macroscopic deformation of the CSK lattice involves microscale motion of molecules over potential energy barriers. These barriers may be intermolecular (e.g., resistance to filament sliding) or intramolecular (e.g., changes in the conformation of

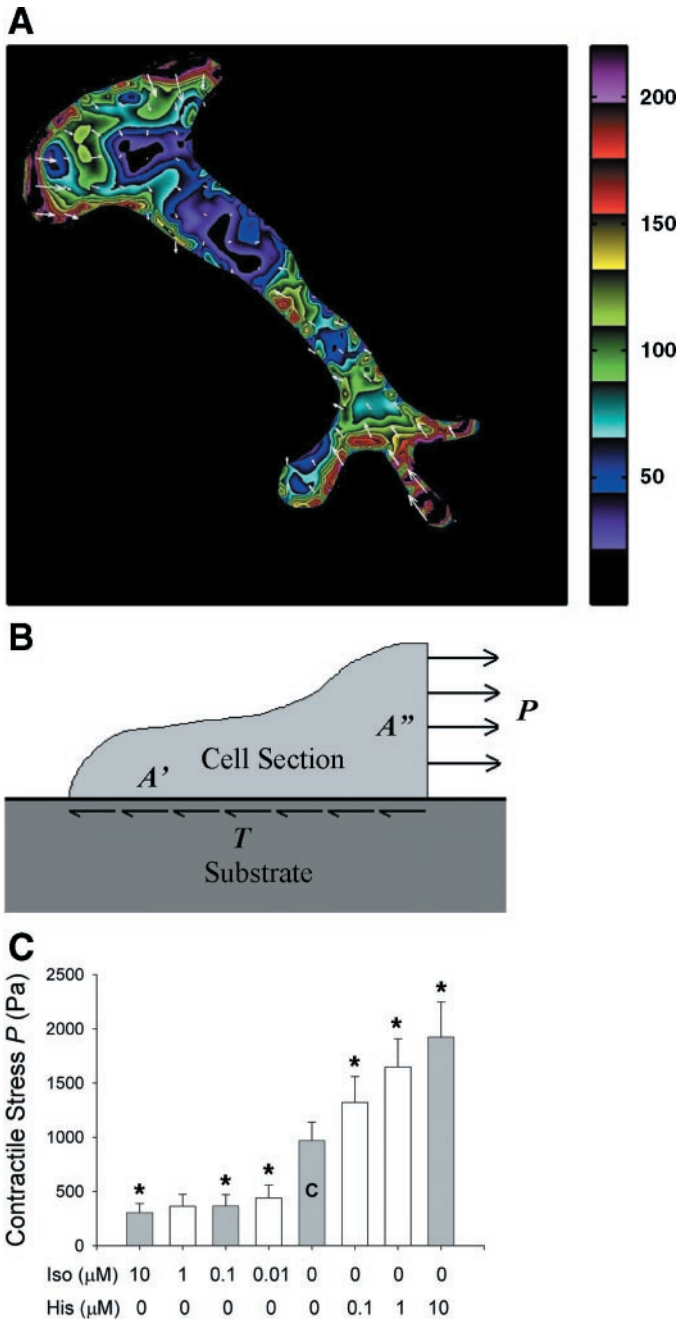

Fig. 2. Fourier transform traction microscopy (3, 25). HASM cells were plated sparsely on a collagen I-coated (0.2 mg/ml) polyacrylamide gel block (70 μm thick). Cell seeding density was similar to the one used during the oscillatory measurements. Many fluorescent microspheres (0.2-μm diameter) were embedded in the gel (the volume fraction of the microspheres in the gel was 1/125). As the cells contracted, displacements of the microspheres were measured. From the measured displacement field and known elastic properties of the gel (Young's modulus of ~1 kPa and Poisson's ratio of 0.45), the traction field was calculated (3). *A*: a traction field distribution for a maximally stimulated cell (10 μM His). White arrows indicate the direction of the traction field. The color code indicates the magnitude of the traction field in Pa (reprinted with permission from Ref. 24). *B*: mean contractile stress (P) was calculated from measurements of mean traction (T) by considering mechanical equilibrium of a free-body diagram of a cell section: $PA'' = TA'$, where A' and A'' are interface (projected) and cross-sectional areas of the cell section, respectively, which are estimated from cell geometry. Calculations were done for a large number of cross sections, and an average value was calculated. *C*: P gradually increases/decreases after graded doses of His/Iso in HASM cells (data taken from Ref. 25). Data are means ± SE; control conditions (C), $n =$ 17 cells; His-treated cells, $n = 13$; and Iso-treated cells, $n = 4$. Shaded bars indicate the doses used in this study in conjunction with the oscillatory data from Fig. 1. *Significantly different from previous dose ($p < 0.05$) calculated relative to the control conditions.

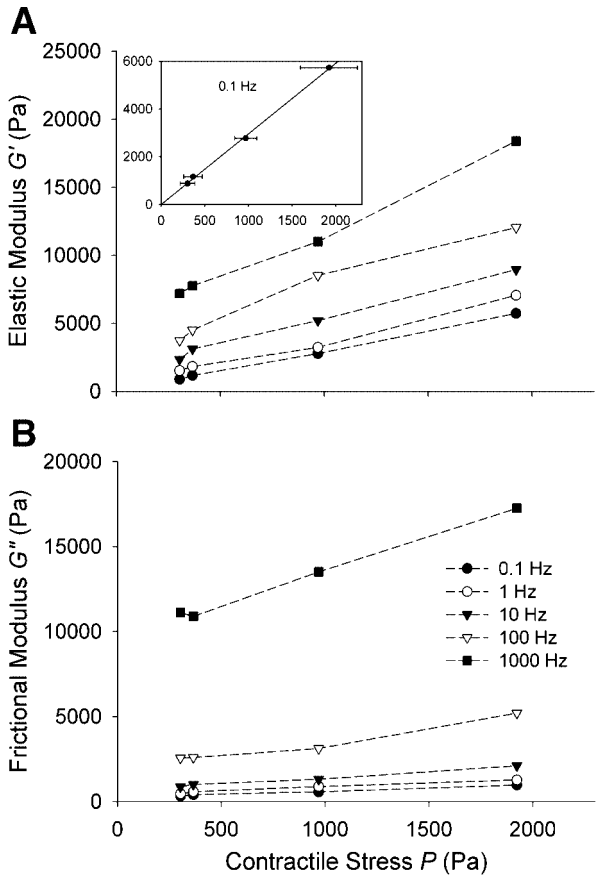

Fig. 3. *A*: G' increased with increasing cytoskeletal P at all frequencies. *Inset*: at 0.1 Hz, G' increased with P in a direct proportion according to *Eq. 2*. Solid line is the fit of *Eq. 2* to the data: $G' = 2.96P$. *B*: G'' also increased with P at all frequencies. Data are means ± SE.

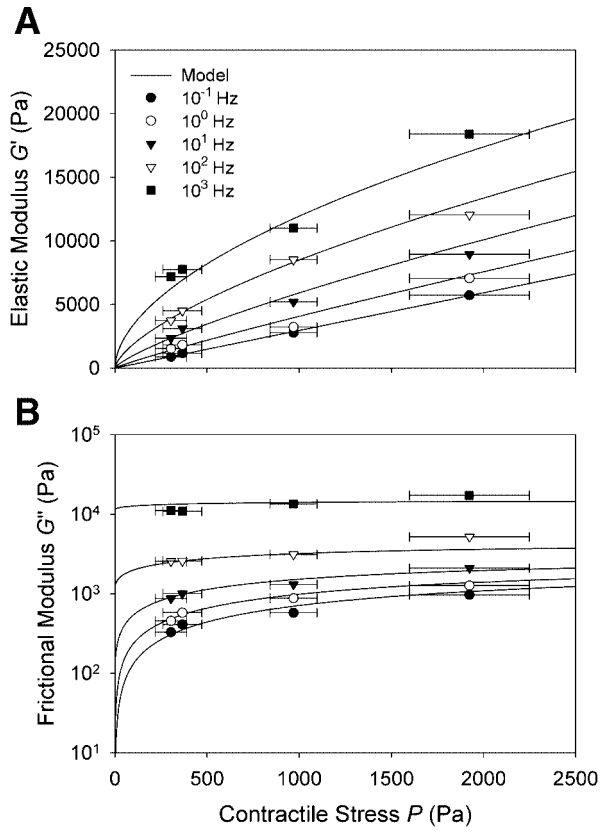

Fig. 5. Empirical relationships for G' (*A*) and G'' (*B*) vs. P for the frequency range of 10^{-1} to 10^{3} Hz, derived from *Eqs. 1* and *3* (lines) were in good agreement with experimental data (dots). Data are means ± SE.

the molecular chain). It has been shown (cf. Ref. 9) that the relationship between the macroscopic flow ($\dot{\epsilon}$) and the applied stress (σ) is given as $\dot{\epsilon} \propto \sigma\exp(-\Delta H/k\theta)$, where ΔH indicates the potential energy barrier, k is the Boltzman's constant, and θ is the absolute temperature. The physics of molecular motion over energy barriers is also known as the Eyring energy activation process (cf. Ref. 12). In the limit of $\Delta H \rightarrow \infty$, i.e., very high energy barrier, $\dot{\epsilon} \rightarrow 0$ (i.e., no flow) implies the solid-like behavior. In the limit of $\Delta H \rightarrow 0$, i.e., very low energy barrier, $\dot{\epsilon}\ \alpha\ \theta$ (i.e., proportionality between stress and flow) which in turn, implies Newtonian fluid-like behavior. Thus, analogous to α in the structural damping model, ΔH in the energy activation model is an index of transition between solid-like and fluid-like behavior. Because our findings show that α changes with P (Fig. 5*A*), we speculate that ΔH may also change with P. An increase in P within the CSK lattice (mainly due to actomyosin cross-bridge formation) may increase the potential energy level of the CSK lattice. One reason could be that, under contractile stress, long chain molecules of the actin CSK network become taut like guitar strings, which, in turn, reduces their effective flexibility. A decrease in flexibility of these molecules increases the effective energy barrier associated with their conformational changes. Thus modulations of the contractile stress might change the level of potential energy barriers within the CSK and thereby alter the cell transition between fluid-like and solid-like cell behavior. Furthermore, it has also been shown that molecular motion over energy barriers may lead to rheological behavior, which is consistent with power-law behavior (cf. Ref. 9). Thus the physics of molecular motion over energy barriers may serve as a good basis for explaining the empirical link between the CSK contractile stress and the cell rheological behavior given by *Eq. 3*.

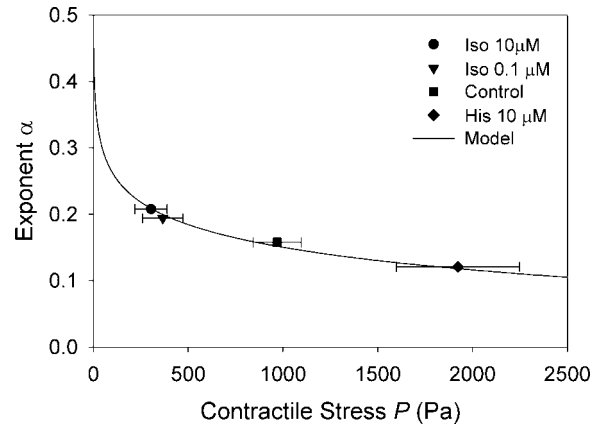

Fig. 4. *A*: power-law exponent (α) decreased with increasing cytoskeletal P. The empirical relationship calculated from *Eq. 3* (line) was in agreement with experimental data (dots). Data are means ± SE.

There are other energy activation theories that could explain the transition between solid and liquid states. One of them is the soft glass rheology proposed by Sollich (18). In this theory,

however, the activation energy is thought to be greater than the thermal energy associated with the Brownian motion. This theory has been successful in explaining the oscillatory behavior of various cell types (6, 7). However, the physical origin of the energy activation processes described in this theory has not yet been fully identified in the CSK.

The transition between solid-like and fluid-like cell behavior is often framed in the context of a gel-sol transition (11, 22, 23). Gels near a critical gelation point exhibit power-law phenomena (12, 16, 26, 27) similar to that observed in soft glasses near a glass transition (18) and the data reported here (Fig. 1). In that connection, it is important to note that both the glass transition and critical gelation are thought to arise from a common mechanism, namely, kinetic arrest due to crowding of clusters, which is a manifestation of more general jamming transitions (17). Recent findings indicate that agonist-induced actin polymerization may not be sufficient to explain the observed stiffening response of smooth muscle cells, however, and that myosin activation is also needed to account for the stiffening (2).

Finally, it is important to point out that phenomena, which have been observed in reconstituted actin networks with myosin II dispersed in them, fail to explain results obtained in living cells. In such reconstituted systems, activation of dispersed myosin by ATP causes fluidization of entangled actin polymer gels and a dramatic reduction of matrix stiffness (10). This result is opposite in sign from the results obtained in living HASM cells, which exhibit stiffening when molecular motors are activated in response to stimulation by histamine (Fig. 3). A possible explanation for this discrepancy is that, within the polymerized actin gel, myosin activation does not induce contractile stress because there are no sites for mechanical anchorage that could counterbalance this stress. Instead, the force generated by the molecular motors pushes the actin filaments through the network, thereby enhancing their longitudinal motion and thus causing an apparent increase in gel fluidity (10). On the other hand, in living cells, the contractile force generated by the molecular motors is transmitted by the actin network to stress fibers, microtubules, and, ultimately, via focal contacts to the extracellular matrix, which counterbalance these forces and thus stabilize the CSK (20, 25). Thus contractile stress enhances stability rather than induces fluidity of the CSK of intact living cells.

In conclusion, we have shown in this study that mechanical stability and rheology of the CSK matrix are linked through the agency of CSK contractile stress. Although the physical basis for this finding remains to be explained, it suggests the possibility that CSK contractile stress may regulate transition between solid-like and fluid-like cell behavior. Activated processes, which have been used to explain rheology of polymer networks, may serve as a basis for explaining the role of the contractile stress in cell transition between solid-like and fluid-like behavior. Results of this study may provide a new perspective on a number of cellular functions that are critically dependent on cell contractility and cell rheology and may set the stage for further investigations in these areas.

ACKNOWLEDGMENTS

Present address of Dr. B. Fabry: Fridrich-Alexander-University of Erlangen, Turnstrasse 5, D-91054 Erlangen, Germany.

GRANTS

This work was supported by National Heart, Lung, and Blood Institute Grants HL-33009 and HL-59215.

REFERENCES

1. **Alfrey T Jr.** *Mechanical Behavior of High Polymers*. New York: Interscience, 1948.
2. **An SS, Laudadio RE, Lai J, Rogers RA, and Fredberg JJ.** Stiffness changes in cultured airway smooth muscle cells. *Am J Physiol Cell Physiol* 283: C792–C801, 2002.
3. **Butler JP, Tolić-Nørrelykke IM, Fabry B, and Fredberg JJ.** Estimating traction fields, moments, and strain energy that cells exert on their surroundings. *Am J Physiol Cell Physiol* 282: C595–C605, 2002.
4. **Csete ME and Doyle JC.** Reverse engineering of biological complexity. *Science* 295: 1664–1669, 2002.
5. **Djordjević VD, Jarić J, Fabry B, Fredberg JJ, and Stamenović D.** Fractional derivatives embody essential features of cell rheological behavior. *Ann Biomed Eng* 31: 692–699, 2003.
6. **Fabry B, Maksym GN, Butler JP, Glogauer M, Navajas D, and Fredberg JJ.** Scaling the microrheology of living cells. *Phys Rev Lett* 87: 148102, 2001.
7. **Fabry B, Maksym GN, Butler JP, Glogauer M, Navajas D, Taback NA, Millet EJ, and Fredberg JJ.** The scale and other invariants of integrative mechanical behavior in living cells. *Phys Rev E Stat Nonlin Soft Matter Phys* 68: 041914, 2003.
8. **Fredberg JJ and Stamenović D.** On the imperfect elasticity of lung tissue. *J Appl Physiol* 67: 2408–2419, 1989.
9. **Halsey G, White HJ Jr, and Eyring H.** Mechanical properties of textiles, I. *Text Res J* 15: 295–311, 1945.
10. **Humphrey D, Duggan C, Saha D, Smith D, and Käs J.** Active fluidization of polymer networks through molecular motors. *Nature* 416: 413–416, 2002.
11. **Janmey PA, Hvidt S, Lamb J, and Stossel TP.** Resemblance of actin-binding protein actin gels of covalently cross-linked networks. *Nature* 345: 89–92, 1990.
12. **Larson RG.** *The Structure and Rheology of Complex Fluids*. New York: Oxford Univ. Press, 1999, p. 238–243.
13. **Lazan B.** *Damping of Materials and Members in Structural Mechanics*. Oxford, UK: Pergamon, 1968.
14. **Mijailovich SM, Kojic M, Zivkovic M, Fabry B, and Fredberg JJ.** A finite element model of cell deformation during magnetic bead twisting. *J Appl Physiol* 93: 1429–1436, 2002.
15. **Panettieri RA Jr, Murray RK, DePalo LR, Yadvish RA, and Kotlikoff MI.** A human airway smooth muscle cell line that retains physiological responsiveness. *Am J Physiol Cell Physiol* 256: C329–C335, 1989.
16. **Scanlan JC and Winter HH.** Composition dependence of the viscoelasticity of end-linked poly(dimethylsiloxane) at the gel point. *Macromolecules* 24: 47–54, 1991.
17. **Sergè PN, Prasad V, Schofield AB, and Weitz DA.** Glasslike kinetic arrest at the colloidal-gelation transition. *Phys Rev Lett* 86: 6042–6045, 2001.
18. **Sollich P.** Rheological constitutive equation for a model of soft glassy materials. *Phys Rev E Stat Nonlin Soft Matter Phys* 58, 738–759, 1998.
19. **Stamenović D and Ingber DE.** Models of cytoskeletal mechanics of adherent cells. *Biomech Model Mechanobiol* 1: 95–108, 2002.
20. **Stamenović D, Mijailovich SM, Tolić-Nørrelykke IM, Chen J, and Wang N.** Cell prestress. II. Contribution of microtubules. *Am J Physiol Cell Physiol* 282: C617–C624, 2002.
21. **Stamenović D and Wang N.** Invited review: Engineering approach to cytoskeletal mechanics. *J Appl Physiol* 89: 2085–2090, 2000.
22. **Stossel TP.** On the crawling of animal cells. *Science* 260: 1086–1094, 1993.
23. **Tempel M, Isenberg G, and Sackmann E.** Temperature induced sol-gel transition and microgel formation in α-actinin cross-linked actin networks: a rheological study. *Phys Rev E Stat Phys Plasmas Fluids Relat Interdiscip Topics* 54: 1802–1810, 1996.
24. **Tolić-Nørrelykke IM, Butler JP, Chen J, and Wang N.** Spatial and temporal traction response in human airway smooth muscle cells. *Am J Physiol Cell Physiol* 283: C1254–C1266, 2002.
25. **Wang N, Tolić-Nørrelykke IM, Chen J, Mijailovich SM, Butler JP, Fredberg JJ, and Stamenović D.** Cell prestress. I. Stiffness and prestress are closely associated in contractile adherent cells. *Am J Physiol Cell Physiol* 282: C606–C616, 2002.
26. **Winter HH.** Polymer gels, materials that combine liquid and solid properties. *MRS Bull* 16: 44–47, 1991.
27. **Winter HH and Mours M.** Rheology of polymers near liquid-solid transitions. *Adv Polym Sci* 134: 165–234, 1997.